Research article

SURFACE and INTERFACE ANALYSIS

Received: 27 August 2012 Revised: 13 November 2012 Accepted: 27 November 2012 Published online in Wiley Online Library 26 December 2012

(wileyonlinelibrary.com) DOI 10.1002/sia.5204

Characterization of surface composition on Alloy 22 in neutral chloride solutions

Dmitrij Zagidulin,[a] Xiangrong Zhang,[a] Jigang Zhou,[b] James J. Noël[a] and David W. Shoesmith[a]*

The composition of anodically grown oxide films on Alloy 22, a Ni-Cr-Mo(W) alloy, has been investigated in 5 mol l^{-1} NaCl at room temperature using X-ray photoelectron spectroscopy and time-of-flight secondary ion mass spectrometry. For applied potentials up to 0.2 V (vs Ag/AgCl (saturated KCl solution)), a Cr(III) oxide barrier layer develops at the alloy/oxide interface accounting for the excellent passivity demonstrated to prevail in this potential region by previous electrochemical impedance spectroscopy measurements. At higher potentials, this layer is destroyed by defect injection as Cr(III) is oxidized to the more soluble Cr(VI). The overall oxide/hydroxide film thickness is, however, increased as Mo(VI)/W(VI) species accumulate at the oxide solution interface. The potential of 0.2 V at which the barrier layer switches from growth to destruction coincides with the previously demonstrated threshold potential for the initiation of crevice corrosion. Copyright © 2012 John Wiley & Sons, Ltd.

Keywords: Alloy 22; passive film; surface analysis

Introduction

Ni-Cr-Mo alloys are well known to exhibit exceptional corrosion resistance under extreme conditions. These alloys are widely used in a range of industrial applications,[1] and Alloy 22 was recently considered as the corrosion barrier on packages for the permanent disposal of nuclear wastes.[2] This last potential application stimulated many studies on this alloy and, to a lesser degree, other Ni-Cr-Mo alloys, on processes such as intergranular corrosion,[3,4] localized corrosion with an emphasis on crevice corrosion,[5–25] stress corrosion cracking,[26–29] and general passive corrosion.[9,30–35]

Alloy 22 develops a very stable passive film[27,36–39] whose electrical properties have been characterized by electrochemical impedance spectroscopy (EIS).[36–38,40–44] These impedance studies clearly show the potential regions over which passivity develops and within which the film eventually becomes unstable and potentially susceptible to the initiation of localized corrosion, specifically crevice corrosion.[20,23,24] It was claimed, based on a comparison to similar EIS studies on Ni-Cr alloys,[45–47] that the enhanced passivity of Alloy 22 could be attributed to a smaller number of less mobile defects, most likely Cr interstitial ions. The loss of passivity at higher applied potentials was then attributed to a switch from n-type to p-type conductivity when cation vacancies were injected into the Cr(III)-dominated passive film leading to its destruction by Cr(III) oxidation to the more soluble Cr(VI) (as CrO_4^{2-}).[48]

In this paper, we present the results of surface analytical studies designed to link the evolution in impedance properties to changes in passive film composition.

Experimental

All experiments were performed on Alloy 22 (Table 1) supplied by Haynes International, Kokomo, Indiana. Cylindrical samples with a geometrical surface area of 0.785 cm^2 were machined from the plate materials. The cylinders were then drilled and tapped at one end to accommodate a threaded rod of the same material. This allowed electrical connections to be made to electrochemical equipment outside the cell. The specimens were wet polished with a series of SiC papers up to 1200 grit and then polished successively with alumina powder suspensions to a 0.8 μm finish. The specimen analyzed using synchrotron radiation was polished to a 0.05 μm finish. Specimens were then rinsed with copious amounts of Type 1 water (resistivity of 18.2 MΩ cm^{-1}, obtained from a Milli-Q Millipore system) and ultrasonically cleaned for 10 min in either acetone or methanol, and after a final rinsing in ultrapure deionized water, placed in the electrochemical cell.

A standard three-electrode electrochemical cell housed in a Faraday cage was used in all experiments. The auxiliary electrode was Pt (99.95%), and all potential values were measured with, and are reported against, an in-house fabricated saturated Ag/AgCl electrode (SSC, 199 mV vs NHE). The cell was fitted with an outer jacket through which silicon oil or water was circulated from a thermostatic bath (Isotemp 3016H, Fisher Scientific) to control the temperature to 30 ± 1 °C. All experiments were carried out in a 5.0 mol l^{-1} NaCl solution (pH 6 to 8), prepared from reagent grade chemicals with Type 1 water. Solutions were deaerated with ultrahigh purity Ar for ≥60 min prior to starting the experiment and purging maintained throughout each experiment.

The time between electrode preparation and its immersion in solution was minimized to avoid complications due to air

* *Correspondence to: David W. Shoesmith, Surface Science Western and Department of Chemistry, University of Western Ontario, London, Ontario N6A 5B7, Canada. E-mail: dwshoesm@uwo.ca*

a *Surface Science Western and Department of Chemistry, University of Western Ontario, London, Ontario N6A 5B7, Canada*

b *Canadian Light Source Inc, University of Saskatchewan, Saskatoon, Saskatchewan, S7N 0X4, Canada*

SURFACE and INTERFACE ANALYSIS

Table 1. Chemical composition of Alloy 22

Component	Ni	Cr	Mo	W	Fe
Concentration (wt. %)	59	22	13	3	3

oxidation.[23] A period of ~60 min of cathodic cleaning at –1.0 V was required to guarantee a reproducible surface. After this cathodic treatment, the potential was stepped to a film formation potential (E) in the range –0.4 to 0.6 V for 120 min. After anodic oxidation the electrode was removed from the cell, rinsed and ultrasonicated in Type 1 water (2 min), dried in a stream of Ar gas and stored in a desiccator.

XPS analyses were performed using either a Kratos Axis Ultra XPS (Surface Science Western, Western University) or the spherical grating monochromator undulator beamline at the 2.9 GeV third generation Canadian Light Source (CLS, Saskatoon) (SR-XPS). In XPS experiments, a monochromatic Al Kα X-ray source was used. In survey scans, an energy range of 1100 eV, pass energy of 160 eV, step size of 0.5 eV, a sweep time of 180 s and an X-ray spot size 700 by 400 μm were used. For high-resolution spectra, an energy range of 20–40 eV, a pass energy of 20 eV and a step size of 0.1 eV were used. All spectra were analyzed using the CasaXPS software.[49] Peak shifts due to charging were normalized to the C 1 s peak position set to 284.8 eV and spectra corrected using a Shirley background correction.[50] Reported binding energies have an error of 0.35 eV. For SR-XPS, the energy resolution (ΔE/E) of the beamline is 10^{-4} with a flux of $> 10^{11}$ photons/s at the photon energy range of 250 – 1500 eV. The incident photons were set at 30° to the sample. The resolution of the Scienta 100 electron energy analyser was determined to be 0.1 eV at the pass energy of 100 eV used for these experiments. The incident energies used were 700, 1000, 1200 and 1500 eV.

The Cr 2p and Ni 2p high-resolution spectra were fitted using the parameters specified by Biesinger *et al.*[51] and Grosvenor *et al.*[52] The distributions of Mo and W oxidation states were estimated using the Mo 3d and W 4f spectra, respectively. The intensity ratios of the Mo $3d_{5/2}$ – Mo $3d_{3/2}$ and W $4f_{7/2}$ – W $4f_{5/2}$ doublets were set at 3:2 and 4:3, respectively.[53,54] The peak separation for the Mo $3d_{5/2}$ – Mo $3d_{3/2}$ doublet was set to 3.13 eV[55] and the spectra fitted using the parameters defined by Spevack and McIntyre.[44] For the W $4f_{7/2}$ – W $4f_{5/2}$ doublet, the peak separation was set to 2.18 eV,[55] and the spectra fitted using parameters defined by Khyzun and Leftheriotis *et al.*[56,57]

Time-of-flight secondary ion mass spectrometry was performed using an Ion-ToF (GmbH) TOF-SIMS IV single reflect ion mass spectrometer (Surface Science Western, Western University). To minimize molecular dissociation, a Cs^+ sputter beam energy of 0.5 kV and a pulsed 25 kV Bi_3^+ analysis beam were used. The signal intensities were normalized to the sum of all analyzed components. The results were analyzed using IONSPEC and IONIMAGE software.

Results and discussion

Figure 1 shows an example of the survey spectra recorded after polarization at 0 V for 120 min at 30 °C. Peaks for W, Mo, O, Cr, Ni and C are observed. Based on such spectra, the change in elemental composition of the film as a function of potential can be determined (Fig. 2). The W 4f signal was not included in analyses due to its very low intensity. Figure 2 shows that, by

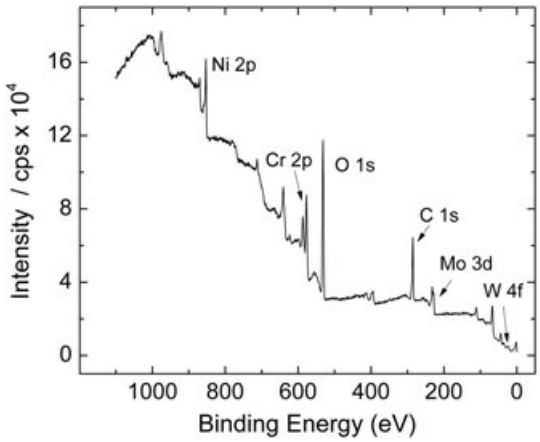

Figure 1. XPS survey spectrum measured on an Alloy 22 surface polarized at 0 V for 120 min. at 30 °C.

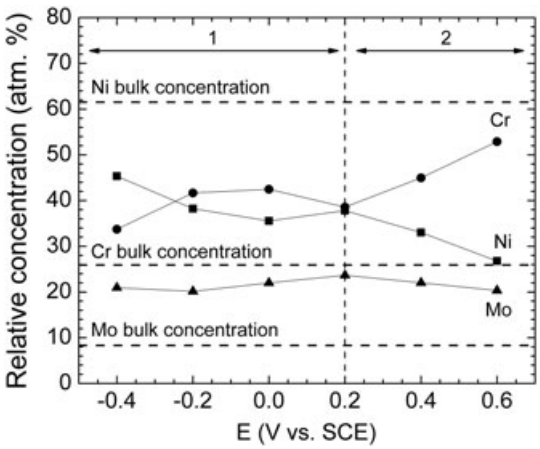

Figure 2. Elemental composition of the film obtained from XPS survey spectra as a function of applied potential. Regions 1 and 2 are defined in the text.

comparison to the composition of the alloy, the film is depleted in Ni and enriched in Cr and Mo.

Two distinct potential regions can be identified, as indicated by the vertical dashed lines in Fig. 2. Over the range –0.4 V to ~ 0.2 V (region 1), the Ni content decreases, and the Cr content increases to plateau values. EIS experiments show this is the potential range over which the passive layer forms achieving maximum resistance over the range –0.1 V to ~ 0.1 V.[23] For potentials more positive than 0.2 V (region 2), the Ni content and Cr content decrease and increase further, respectively. Over this potential range, the film resistance decreases substantially, and the film capacitance increases.[23] By contrast, the total Mo content remains approximately constant over the entire potential range, –0.4 V to 0.6 V.

Based on the fits to a series of high-resolution spectra (as illustrated in Fig. 3), the relative fractions of various species in the electrode surface can be determined as a function of applied potential (Fig. 4). For all elements, the relative concentrations can be divided into the same two distinct potential regions defined in the survey spectra. Over the lower potential range (1), oxidized Ni is present primarily in the oxide as opposed to hydroxide form. For Cr, the high $Cr(OH)_3$ content of the surface in this potential

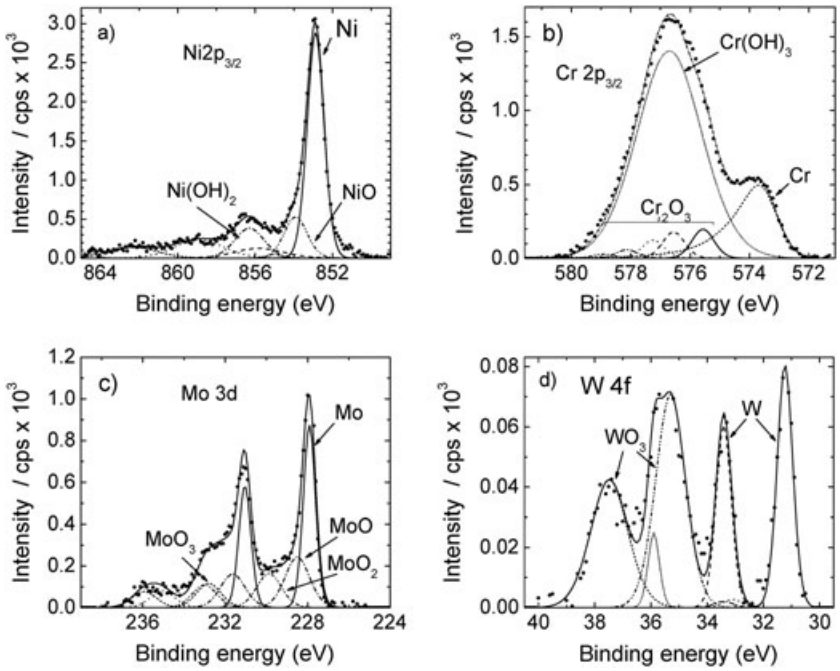

Figure 3. Examples of fitted high-resolution XPS spectra for the (a) Ni2p, (b) $Cr2p_{3/2}$, (c) Mo3d, (d) W4f regions of the spectra. In the examples shown, the applied potential was 0 V.

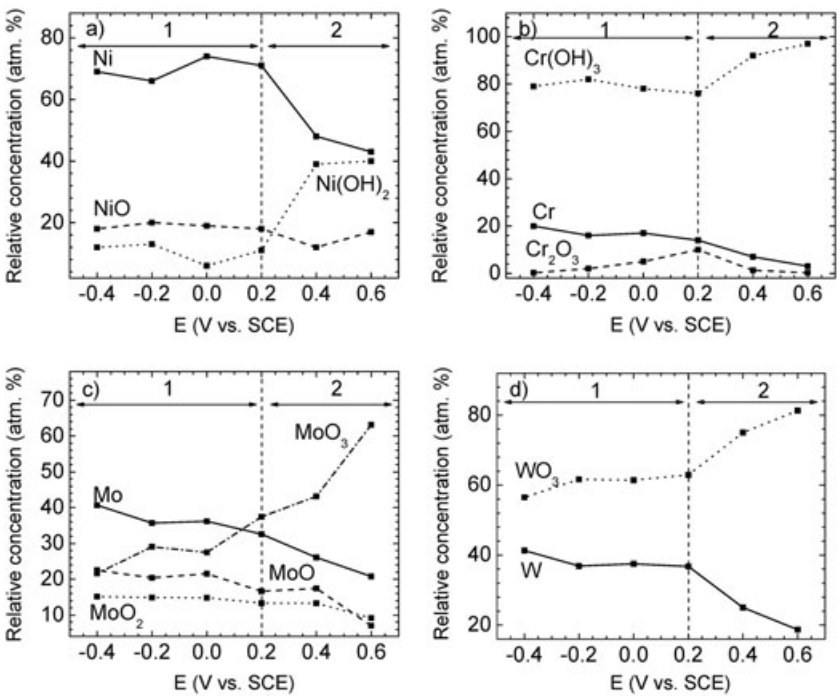

Figure 4. Concentration of Ni(a), Cr(b), Mo(c) and W(d) species in the analyzed surface layer as a function of applied potential (E). Regions 1 and 2 are defined in the text.

range may reflect the prolonged cathodic pretreatment required to produce a reproducible surface prior to the anodic oxidations performed.

Despite this complication, the increased relative concentration of Cr (compared to Ni) in this range (Fig. 3) is accompanied by an increase in Cr_2O_3 content, from ~0 atm.% at –0.4 V to a maximum of ~10 atm.% at 0.2 V. EIS measurements[23] show this increase is accompanied by an increase in film resistance and thickness, with the latter determined from the observed decrease in capacitance over this potential range. These observations are consistent with the generally observed formation of a Cr(III)-dominated barrier layer on Fe-Cr and Ni-Cr alloys.[48,58–60] Also, consistent with EIS measurements, the decreases in relative amounts of all the alloy metallic components (Fig. 4) show the film thickness increases with potential over this range.

Mo is present in a number of oxidation states in this potential range including Mo(II), Mo(IV) and Mo(VI). The possible presence of non-stoichiometric Mo_4O_{11} has been noticed. However, due to partial overlap of the Mo_4O_{11} and MoO_3 signals in the XPS spectra, the presence of Mo_4O_{11} cannot be determined with a high level of confidence. Consequently, Mo_4O_{11} has been excluded from following analysis. The relative concentrations of these components do not appear to be potential dependent over this range. For W, there is a slight increase in WO_3 content. If W(II) is present in the oxide, it is undetectable.

For potentials > 0.2 V, there is a decrease in Cr_2O_3 content and an increase in $Cr(OH)_3$ content. For Ni, $Ni(OH)_2$ becomes the dominant film component, although the survey spectra in Fig. 1 show an overall decrease in Ni content of the film relative to the Cr content. Although the survey spectra show no relative change in the Mo content of the film, there is a very definite increase in oxidized Mo states. A similar increase is observed for W.

EIS measurements show there is a significant decrease in film resistance and increase in film capacitance for potentials 0.2 V[23] consistent with the destruction of the Cr(III)-dominated barrier layer (decreased resistance) and the production of multiple high oxidation states of Mo and W (increased capacitance). Despite the onset of defect injection into the barrier layer leading to its thinning, the decreased contents of all the alloy metallic components indicate an actual increase in overall film thickness. Consistent with measurements on stainless steels,[61,62] despite the overall increase in relative Cr content of the oxide (Fig. 2), Cr(VI) is not detected by XPS. It is possible that this can be attributed to its release to solution although an alternative explanation is offered below.

To investigate the distribution of species in the passive film, SR-XPS spectra were recorded at various excitation energies on a specimen anodically oxidized at 0 V; i.e. at a potential in the passive region. Since the inelastic mean free path depends on the excitation energy of the X-ray beam, depth profiling can be achieved. Surface compositions determined from the survey spectra are shown in Fig. 5. While the increase in Ni content with increasing energy suggests this element is depleted in the outer regions of the film, its very high content at the highest excitation energy (1500 eV) indicates that the analysis reached the substrate alloy. This is confirmed by the high-resolution spectra, (Fig. 6) which exhibits an excitation energy-dependent signal for Ni metal in the Ni $2p_{3/2}$ peak.

The Cr content achieves a maximum at the intermediate excitation energy of 1200 eV which suggests its enrichment in the inner regions of the film close to the oxide/alloy interface. By contrast, the Mo content is at a maximum at the lowest excitation energy (1000 eV) suggesting its enrichment in the outer regions of the film. Although not shown here, fitting of the high-resolution spectra, using the procedure described above, indicate that the Cr in the inner regions of the film is Cr_2O_3.

To confirm the distribution of cations within the oxide film present in potential regions 1 and 2, ToF-SIMS depth profiles were recorded after anodic oxidation at –0.4 V, 0 V and 0.6 V. Figure 7 demonstrates the presence of a dual layer, consistent with the SR-XPS results. At all three potentials, but especially at 0.6 V, the high oxidation states Mo(VI) and W(VI) (MoO_3, WO_3) are segregated to the outer regions of the film along with Cr(III) in the hydroxide form and, although not shown, $Ni(OH)_2$ also.

By contrast, Cr(III) (Cr_2O_3) is retained in the inner regions of the film consistent with the SR-XPS results and the generally observed Cr(III) oxide barrier layer at the alloy/oxide interface in the passive region. Mo(IV) (MoO_2) appears to be distributed uniformly throughout the film with an apparent, but not very obvious, slight concentration in the outer regions near the oxide/solution interface. At all three potentials studied, a dual layer film is observed with Mo(VI) (MoO_3), W(VI) (WO_3), Cr(III) and Ni(II) hydroxides close to, or at, the oxide/hydroxide/solution interface, and Cr(III) (Cr_2O_3), Ni(II) (NiO) and Mo(IV)/W(IV) oxides at the alloy/oxide interface. While absolute film thicknesses remain uncertain, it is clear from the ToF-SIMS depth profiles that the film thickness increases by a factor of 3 to 4 in potential region 2 ($>$ 0.2 V) compared to region 1 consistent with the XPS analyses. Film thickening in this manner requires cation transport through the oxide film and only becomes feasible once the passive layer (shown to be dominantly Cr(III) (Cr_2O_3)) is, at least partially, destroyed by transpassive oxidation of Cr(III) to Cr(VI) (CrO_4^{2-}). The XPS results clearly demonstrate the loss of Cr_2O_3 for potentials > 0.2 V, which would explain the decrease in resistance observed in previous EIS studies over this potential range (1).[23] The increase in film capacitance which accompanies oxidation in the transpassive region (2)[23] can then be attributed to the

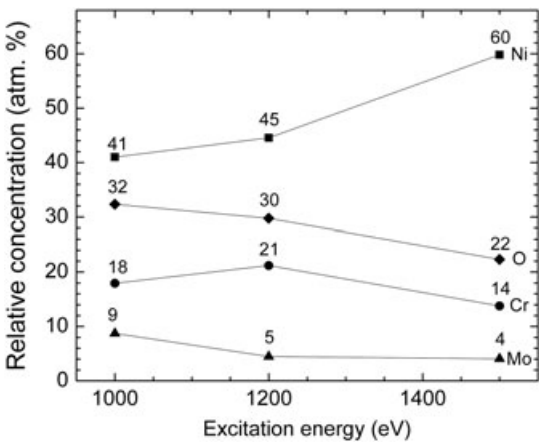

Figure 5. Surface composition determined from the survey spectra recorded on Alloy 22 after polarization at 0 V (pH 7, 44 h) at various incident photon excitation energies (1000, 1200 and 1500 eV).

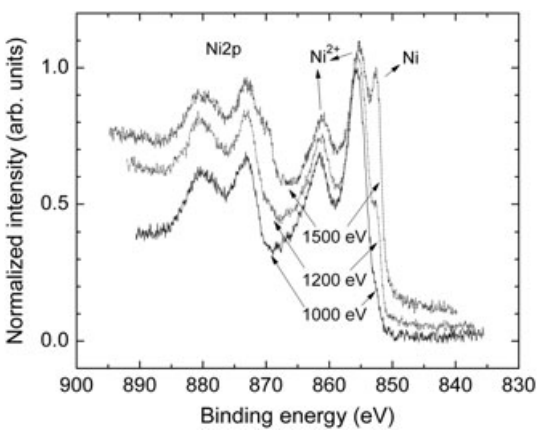

Figure 6. High-resolution Ni 2p XPS spectra recorded on Alloy 22 after polarization at 0 V (pH 7, 44 h) at various incident photon excitation energies (1000, 1200, 1500 eV).

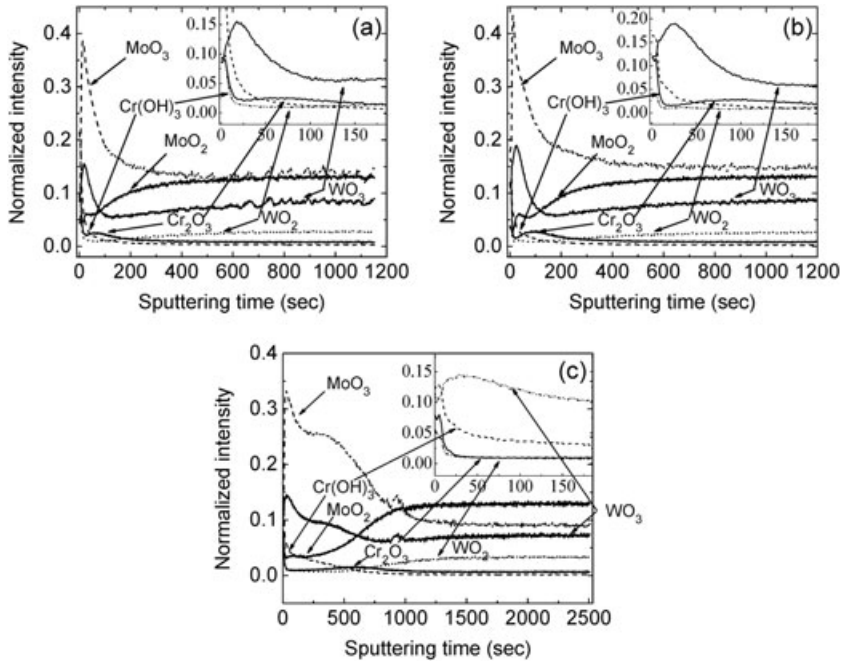

Figure 7. ToF SIMS depth profiles obtained on Alloy 22 after polarization at different applied potentials; (a) –0.4 V, (b) 0 V and (c) 0.6 V.

film thickening and accumulation of Mo(VI) and W(VI) states in the film.

According to both XPS and ToF-SIMS analyses, transpassive oxidation leads to the accumulation of $Cr(OH)_3$. This suggests that destruction of the Cr(III) oxide barrier layer leads to the transport of Cr(III) to the outer regions of the film. This would be inconsistent with the oxidative transformation of this film to produce Cr(VI), a well-documented process.[63–66] However, neither analytical method detects Cr(VI) in the film after transpassive oxidation at 0.6 V. As noted above, this could be partially attributed to the loss of CrO_4^{2-} by dissolution, but is probably equally due to Cr (VI) reduction back to Cr(III) by one or both of two processes. Reduction of Cr(VI) can occur when the electrode is removed from the electrochemical cell and transferred to the UHV system of the analytical instruments.[66] In addition, Cr(VI) reduction can be induced by the X-ray beam when XPS analyses are performed.

The retention of Mo(VI)/W(VI) in the outer regions of the film would not necessarily be expected in neutral solution in which these species are quite soluble. Their accumulation can be attributed to the local production of acidity which will accompany the formation of Cr(VI), Mo(VI) and W(VI) species (e.g. $Cr_2O_3 + 5H_2O + 6e \rightarrow 2CrO_4^{2-} + 10H^+$).

Summary and conclusions

XPS and SR-XPS experiments show that the composition of the passive oxide film on Alloy 22, a Ni-Cr-Mo(W) alloy, varies with applied potential, and ToF-SIMS experiments demonstrate that the composition also varies with depth within the film.

Two distinct potential ranges of behaviour are observed. Over the range –0.4 V to 0.2 V, the passive oxide film thickens and an inner Cr(III) oxide barrier layer is developed. For potentials above 0.2 V, this barrier layer is destroyed, and the film thickens considerably (by a factor of 3 to 4) due to the accumulation of Mo(VI) and W(VI) species in the outer regions of the film at the oxide/solution interface.

These observations are consistent with previously published EIS results which show that this development of the Cr(III) oxide barrier layer (–0.4 V to 0.2 V) is accompanied by an increase in interfacial resistance and a decrease in interfacial capacitance. For potentials > 0.2 V, the destruction of the barrier layer leads to a decrease in resistance and the accumulation of the higher oxidation states of Mo/W to an increase in capacitance.

The decrease in Cr(III) oxide, i.e. the destruction of the protective barrier layer, also coincides with the previously measured potential threshold for the initiation of crevice corrosion on this alloy.

Acknowledgements

This research is funded under the Industrial Research Chair agreement between the Canadian Natural Sciences and Engineering Research Council (NSERC). The authors thank the Science and Technology Program of the Office of the Chief Scientist (OCS), Office of Civilian Radioactive Waste Management (OCRWM) and the United States Department of Energy (DOE) for support. The work was performed under the Corrosion and Materials Performance Cooperative, DOE Cooperative Agreement No. DE-FC28-04RW12252. The views and opinions of the authors expressed herein do not necessarily state or reflect those of the United States Department of Energy.

CLS is supported by NSERC, NRC, CIHR and the University of Saskatchewan.

References

[1] R. Rebak, in *Corrosion and Environmental Degradation* (Ed.: M. Schutze), Wiley-VCH, **2000**, pp. 69.
[2] G. M. Gordon, *Corrosion 2002* **2002**, *58*, 811.

[3] K. S. Raja, S. A. Namjoshi, D. A. Jones, *Metall. Mater. Trans. A* **2005**, *36A*, 1107.
[4] D. D. Gorhe, K. S. Raja, S. A. Namjoshi, V. Radmilovic, A. Tolly, D. A. Jones, *Metall. Mater. Trans. A* **2005**, *36A*, 1153.
[5] D. S. Dunn, L. Yang, C. Wu, G. A. Cragnolino, in Materials Research Society Symposium **2004**, pp. 33.
[6] S. D. Day, M. T. Whalen, K. J. King, G. A. Hust, L. L. Wong, J. C. Estill, R. B. Rebak, *Corrosion (Houston, TX, U. S.)* **2004**, *60*, 804.
[7] D. D.Macdonald, G. Engelhardt, P. Jayaweera, N. Priyantha, A. Davydov, *European Federation of Corrosion Publications* **2003**, *36*, 103.
[8] B. A. Kehler, G. O. Ilevbare, J. R. Scully, in *Corrosion 2001*, *Vol. 57*, **2001**, pp. 1042.
[9] K. J. Evans, A. Yilmaz, S. D. Day, L. L. Wong, J. C. Estill, R. B. Rebak, *JOM* **2005**, *57*, 56.
[10] D. S. Dunn, Y. M. Pan, K. T. Chiang, L. Yang, G. A. Cragnolino, X. He, *JOM* **2005**, *57*, 49.
[11] V. Jain, D. Dunn, N. Sridhar, L. Yang, Corrosion 2003 **2003**, *Paper No. 03690*.
[12] D. S. Dunn, L. Yang, Y. M. Pan, G. A. Cragnolino, Corrosion 2003 **2003**, *Paper No. 03697*.
[13] R. B. Rebak, Corrosion 2005 **2005**, *Paper No. 05610*.
[14] A. K. Mishra, G. S. Frankel, *Corrosion (Houston, TX, U. S.)* **2008**, *64*, 836.
[15] M. R. Ortíz, M. A. Rodríguez, R. M. Carranza, R. B. Rebak, *Corrosion (Houston, TX, U. S.)* **2010**, *66*, 105002.
[16] C. M. Giordano, M. R. Ortíz, M. A. Rodríguez, R. M. Carranza, R. B. Rebak, *Corros. Eng., Sci. Technol.* **2011**, *46*, 129.
[17] R. M. Carranza, M. A. Rodríguez, R. B. Rebak, *Corrosion (Houston, TX, U. S.)* **2007**, *63*, 480.
[18] X. He, B. Brettman, H. Jung, *Corrosion (Houston, TX, U. S.)* **2009**, *65*, 449.
[19] M. A. Rodríguez, R. M. Carranza, R. B. Rebak, *Corrosion (Houston, TX, U. S.)* **2010**, *66*, 015007.
[20] P. Jakupi, D. Zagidulin, J. J. Noël, D. W. Shoesmith, *Electrochemical Society Transactions* **2006**, *3*, 259.
[21] P. Jakupi, J. J. Noël, D. W. Shoesmith, *Electrochem. Solid-State Lett.* **2010**, *13*, C1.
[22] P. Jakupi, F. Wang, J. J. Noël, D. W. Shoesmith, *Corros. Sci.* **2011**, *53*, 1670.
[23] P. Jakupi, D. Zagidulin, J. J. Noël, D. W. Shoesmith, *Electrochim. Acta* **2011**, *56*, 6251.
[24] P. Jakupi, J. J. Noël, D. W. Shoesmith, *Corros. Sci.* **2011**, *53*, 3122.
[25] P. Jakupi, J. J. Noël, D. W. Shoesmith, *Corros. Sci.* **2012**, *54*, 260.
[26] P. L. Andresen, G. M. Gordon, S. C. Lu, *JOM* **2005**, *57*, 27.
[27] P. L. Andresen, L. M. Young, G. M. Catlin, P. W. Emigh, G. M. Gordon, *Metall. Mater. Trans. A* **2005**, *36A*, 1187.
[28] G. A. Cragnolino, D. S. Dunn, Y. M. Pan, in Materials Research Society Symposium Proceedings, **2004**, pp. 435.
[29] Y. M. Pan, D. S. Dunn, L. Yang, G. A. Cragnolino, in Materials Research Society Symposium Proceedings, **2002**, pp. 743.
[30] A. C. Lloyd, R. J. Schuler, J. J. Noël, D. W. Shoesmith, F. King, in Materials Research Society Symposium Proceedings, **2004**, pp. 3.
[31] A. C. Lloyd, D. W. Shoesmith, J. J. Noël, N. S. McIntyre, in *Proceedings of the International Symposium on Environmental Degradation of Materials and Corrosion Control in Metals*, Vancouver, BC, Canada, **2003**, pp. 31.
[32] A. C. Lloyd, D. W. Shoesmith, N. S. McIntyre, J. J. Noël, *J. Electrochem. Soc.* **2003**, *150*, B120.
[33] A. C. Lloyd, J. J. Noël, N. S. McIntyre, D. W. Shoesmith, *JOM* **2005**, *57*, 31.
[34] J. R. Hayes, A. W. Szmodis, K. L. Anderson, C. A. Orme, Corrosion 2004 **2004**, Paper No. 04697.
[35] T. Lian, J. C. Estill, G. A. Hust, R. B. Rebak, Corrosion 2003 **2003**, *Paper No. 03694*.
[36] J. J. Gray, J. R. Hayes, G. E. Gdowski, B. E. Viani, C. A. Orme, *J. Electrochem. Soc.* **2006**, *153*, B61.
[37] J. J. Gray, J. R. Hayes, G. E. Gdowski, C. A. Orme, *J. Electrochem. Soc.* **2006**, *153*, B156.
[38] M. A. Rodríguez, R. M. Carranza, R. B. Rebak, *J. Electrochem. Soc.* **2010**, *157*, C1.
[39] M. A. Rodríguez, R. M. Carranza, R. B. Rebak, *Metall. Mater. Trans. A.* **2005**, *36A*, 1179.
[40] J. J. Gray, C. A. Orme, *Electrochim. Acta* **2007**, *52*, 2370.
[41] D. D.Macdonald, A. Sun, N. Priyantha, P. Jayaweera, *J. Electroanal. Chem.* **2004**, *572*, 421.
[42] N. Priyantha, P. Jayaweera, D. D. Macdonald, A. Sun, *J. Electroanal. Chem.* **2004**, *572*, 409.
[43] D. D. Macdonald, A. Sun, *Electrochim. Acta* **2006**, *51*, 1767.
[44] P. A. Spevack, N. S. McIntyre, *J. Phys. Chem.* **1993**, *97*, 11020.
[45] M. Bojinov, P. Kinnunen, G. Sundholm, *Corrosion (Houston, TX, U. S.)* **2003**, *59*, 91.
[46] M. Bojinov, G. Fabricius, P. Kinnunen, T. Laitinen, K. Mäkelä, T. Saario, G. Sundholm, *J. Electroanal. Chem.* **2001**, *504*, 29.
[47] M. Bojinov, A. Galtayries, P. Kinnunen, A. Machet, P. Marcus, *Electrochim. Acta* **2007**, *52*, 7475.
[48] P. Marcus, V. Maurice, in *Passivity and Its Breakdown* (Eds.: P. Natishan, H. Isaacs, M. Janik-Cjachor, V. Macagno, P. Marcus, M. Seo), The Electrochemical Society, Pennington, New Jersey, USA, **1998**.
[49] Internet Communication **2006**.
[50] B. S. Norgren, M. A. J. Somers, J. H. W. Dewit, *Surf. Interface Anal.* **1994**, *21*, 378.
[51] M. C. Biesinger, C. Brown, J. R. Mycroft, R. D. Davidson, N. S. McIntyre, *Surf. Interface Anal.* **2004**, *36*, 1550.
[52] A. P. Grosvenor, M. C. Biesinger, R. S. Smart, N. S. McIntyre, *Surf. Sci.* **2006**, *600* 1771.
[53] D. Briggs, M. P. Seah, *Practical surface analysis by auger and photoelectron spectroscopy*, John Wiley & Sons, Toronto, **1983**.
[54] J. I. Jeong, J. H. Hong, J. H. Moon, J. S. Kang, Y. Fukuda, *J. Appl. Phys.* **1996**, *79* 9343.
[55] J. F. Moulder, W. F. Stickle, P. E. Sobol, K. D. Bomben, *Handbook of X-ray Photoelectron Spectroscopy*, Perkin-Elmer Corporation Physical Electronics Division, Eden Prairie, **1992**.
[56] O. Y. Khyzhun, J. Alloys *Compd.* **2000**, *305*, 1.
[57] G. Leftheriotis, S. Papaefthimiou, P. Yianoulis, A. Siokou, D. Kefalas, *Appl. Surf. Sci.* **2003**, *218*, 276.
[58] P. Marcus, V. Maurice, in *Corrosion and Environmental Degradation* (Ed.: M. Schutze), Wiley-VCH, New York, **2000**.
[59] V. Maurice, W. Yang, P. Marcus, *J. Electrochem. Soc.* **1994**, *141*, 3016.
[60] V. Maurice, W. Yang, P. Marcus, *J. Electrochem. Soc.* **1996**, *143*, 1182.
[61] P. Marcus, J. M. Grimal, *Corros. Sci.* **1992**, *33*, 805.
[62] V. Maurice, W. P. Yang, P. Marcus, *J. Electrochem. Soc.* **1998**, *145*, 909.
[63] P. Schmuki, S. Virtanen, A. J. Davenport, C. M. Vitus, *J. Electrochem. Soc.* **1996**, *143*, 3997.
[64] M. Bojinov, G. Fabricius, T. Laitinen, K. Makela, T. Saario, G. Sundholm, *Electrochim. Acta* **2000**, *45*, 2029.
[65] M. Bojinov, G. Fabricius, T. Laitinen, T. Saario, *J. Electrochem. Soc.* **1998**, *145*, 2043.
[66] J. A. Bardwell, G. I. Sproule, B. Macdougall, M. J. Graham, A. J. Davenport, H. Isaacs, *J. Electrochem. Soc.* **1992**, *139*, 371.

